This is a preprint, the final version is subject to change, of the American Mineralogist (MSA)
Cite as Authors (Year) Title. American Mineralogist, in press.
(DOI will not work until issue is live.) DOI: http://dx.doi.org/10.2138/am-2017-6170

Revised version 1

Previously unknown mineral-nanomineral relationships with important environmental consequences: The case of chromium release from dissolving silicate minerals

Michael Schindler[1]*, Debora Berti[2] and Michael F. Hochella Jr.[3,4]

1. Department of Earth Sciences, Laurentian University, Sudbury, ON
2. NanoEarth, Institute for Critical Technology and Applied Science, Virginia Tech, Blacksburg, VA, 24061, USA
3. Department of Geosciences, Virginia Tech, Blacksburg, VA, 24061, USA
4. Geosciences Group, Pacific Northwest National Laboratory, Richland, WA, 99352, USA

*corresponding author: mschindler@laurentian.ca

ABSTRACT

Risk assessments that take into account the formation of environmentally dangerous hexavalent chromium in Cr-containing mine tailings, and associated soils and sediments, require an understanding of the occurrence and speciation of Cr in silicate minerals and glasses. Silicates are more soluble and generally more susceptible to weathering than the refractory mineral chromite, the principal ore mineral of Cr. Studies at the nanoscale using a combination of advanced sample preparation via microtoming and focused ion beam techniques, in combination with state-of-the art analytical transmission electron microscopy and electron diffraction, reveal the occurrence of chromite nanoparticles held within clinochlore and lizardite grains within chromitite ore (an igneous cumulate consisting primarily of chromite) from the Black Thor Chromium deposit in Northern Ontario, Canada and the Mistake Mine, Fresno County, California, USA, respectively. Nano-scale examinations of altered chromitite ore samples from the Black Thor deposit after dissolution experiments in sulfuric acid-bearing solutions of pH 2.5 show that clinochlore alters to amorphous silica depleted in chromite nanoparticles. This observation suggests the release of chromite nanoparticles rather than Cr^{3+} aqueous species during the weathering of chromite-bearing silicate minerals. This will in turn have an impact on the environmental behavior of Cr^{3+} and its potential oxidation to Cr^{6+}. The formation of Cr^{6+}_{aq} species in this case will require either the initial dissolution of the nanoparticles or the oxidation of Cr^{3+} species on the surface of the nanoparticles, either process being a rate limiting step in the formation of Cr^{6+}_{aq} species.

INTRODUCTION

Chromium can be potentially harmful in the environment as a result of industrial waste mismanagement, accidental spills, and the presence of Cr-bearing rocks and minerals in aquifers, soils, mines, and mine waste. In ultramafic rocks, Cr is present as Cr^{3+} which has relatively low toxicity, is a micronutrient, and is relatively insoluble and immobile at neutral to alkaline pH. In contrast, Cr^{6+} is an environmental toxin and human carcinogen (Fendorf, 1995 and references therein) and is highly mobile at neutral to alkaline pH. Chromium (III) can be readily oxidized to Cr^{6+} by naturally occurring $Mn^{3+/4+}$-oxides (e.g., Bartlett and James, 1979; Eary and Rai, 1987; Fendorf, 1995; Weaver and Hochella, 2003; Oze et al., 2007). Hexavalent Cr can be reduced by organic carbon, bacteria, sulfides and Fe^{2+} (e.g. Kamaludeen et al., 2003, and references therein).

Several studies have focused on the Cr chemistry and mineralogy of serpentinite and serpentine-derived soils as Cr-bearing silicates of the serpentine and chlorite-groups are more susceptible to weathering than the refractory mineral chromite (e.g., Fandeur et al., 2009; Hseu and Iizuka, 2013; Oze et al., 2004, 2007; Morrison et al. 2015). Elevated Cr^{6+} concentrations in soil pore water and groundwater adjacent to serpentinite have been reported (e.g. Izbicki et al., 2008; Wood et al., 2010). In other locations, spectroscopic studies on the speciation of Cr in serpentine-derived soils indicated the absence of detectable amounts of Cr^{6+} (Hseu and Lizuka 2013; Fandeur et al. 2009).

Nanoparticles (NPs) are known to adsorb and/or structurally incorporate problematic metallic contaminants, highly actively and efficiently, from their immediate environment and transport them over vast distances via fluvial and alluvial processes (e.g., Hochella et al., 2005; Plathe et al. (2010); Yang et al 2015). Therefore, it is also likely that, the occurrence of nano-size refractory minerals such as chromite, if present as is the case here (see below), play a significant role in dictating the transport, distribution, bioavailability, and toxicity of Cr in the environment. These phenomena will be particularly critical in areas around mine tailings and

chromite-rich soils and sediments down hydrologic gradient. We will show in this study that Cr occurs in the form of chromite NPs which are encapsulated within silicate minerals of the recently discovered large chromite deposits in the McFaulds Lake greenstone belt in northern Ontario, Canada (i.e. the Black Label, Black Thor and Big Daddy chromite deposits; Laarman 2013, Weston and Shinkle, 2013) and the well-known Mistake Mine, New Idria district, Fresno, California, USA. The presence of chromite NPs in Cr-rich silicate minerals will have significant implications with respect to our understanding of the mobility of Cr and its retention in soils derived from Cr-rich ultramafic rocks.

The strategy used in this study was to assess samples from the two geographically and geologically distinct chromite ore deposits mentioned above to look at solid state Cr distribution in both the fresh ore, and (in the case of the Black Thor ore) simulated acid-mine drainage (AMD) weathered sample capable of releasing Cr into the surrounding environment. In this study, both the fresh and acid-etched ore came from the same sample obtained by placing a fresh ore block into an acidic solution (pH 2.5) for one month. Sampling the edge of the block proved to be sufficient to observe both altered and unaltered minerals. This resulted in excellent control for sampling for the Cr-state of the ore from fresh to an acid-etched, weathered condition.

The two starting materials were as follows: 1) High grade chromitite ore samples were obtained from the Black Thor chromite ore deposit, Ontario, Canada, through the Ontario Geological Survey. The deposit occurs within a regional volcanic-intrusive complex known as the ‘Ring of Fire’ ultramafic-mafic intrusive suite (Weston and Shinkle, 2013). 2) A chromitite ore sample was also obtained from the Mistake Mine, New Idria district, Fresno, California, USA through the Natural History Museum of Los Angeles Count (catalogue No. NHMCAL: 36235). The chromite is hosted by serpentinites which are part of the Franciscan Complex, a complex of metamorphosed ophiolitic rocks uplifted along the subduction zone of the oceanic crust and the continental crust of the North American Plate (Coleman, 1996).

METHODS

Details on the dissolution experiments, scanning electron microscopy (SEM) and transmission electron microscopy (TEM) studies as well as additional EDS chemical distribution maps recorded scanning TEM mode (STEM), the location of the extracted focused ion beam sections and selected area electron diffractions pattern (SAED) of all identified phases are listed in the Supplementary Information section (Figures S1-S10).

RESULTS

The chromitite samples from the Black Thor deposit and the Mistake Mine, California, contain the Cr-rich silicates clinochlore, $Mg_3[Si_4O_{10}(OH)_2]$ x $(MgAl_{1.33}(OH)_6)$ and lizardite, $(Mg_{2.3}Al_{0.46})Si_2O_5(OH)_4$ which occur in the interstitials between rounded grains of chromite (Fig.1.). The Cr-content in these silicates is on average 3 and 1 wt% Cr, respectively. The chromites from both deposits are Mg- and Al-rich as follows: $(Fe_{0.5}Mg_{0.5})(Al_{0.6}Cr_{1.4}O_4)$, Black Thor; and $(Mg_{0.7}Fe_{0.3})(Al_{0.4}Cr_{1.6}\ O_4)$, Mistake Mine, de facto magnesiochromite.

TEM images and EDS chemical distribution maps for Cr indicate the occurrence of chromite NPs within Cr-rich clinochlore and lizardite from the Black Thor deposit and Mistake Mine, respectively (Fig. 1b-f, S3). The NPs can be distinguished in bright field TEM images from the silicate matrix on the basis of their darker color, being less electron beam transparent (Fig. 1b, 1f), and a characteristic d-spacing of their lattice fringes (Fig. 1c, f). The presence of chromite NPs in clinochlore can also be recognized in SAED patterns in which diffraction spots indicate the presence of a single crystal of clinochlore, whereas diffuse diffraction rings represent exceptionally small chromite NPs (generally less than 3-5 nm) in random orientations (Fig. 1d). Larger chromite particles also occur in the Cr-rich lizardite matrix (Fig. 1e) in which nano-size fragments of different orientations and sizes are intergrown (Fig. S10).

After the dissolution experiment, the chromite from the Black Thor deposit is weakly altered displaying only rarely any etch features or secondary mineral coatings on their surface

(Fig. S1). Conversely, areas composed of clinochlore are strongly altered and are often characterized by surface coatings enriched in Si and depleted in Mg and Al. The absence of diffraction spots and rings in SAED patterns taken from silica-rich areas in the FIB section extracted from the surface of the altered chromitite indicate the occurrence of an amorphous silica modification (Fig. S5). TEM images indicate the occurrence of fragments of clinochlore in areas composed of mainly amorphous silica (Fig. 2a-d). Chemical distribution maps (Fig. 2c-e), TEM images (Figs. 2a-b) and SAED pattern (Fig. S5) indicate a higher abundance of chromite NPs (and thus Cr concentrations) in clinochlore fragments and in areas containing clinochlore fragments than in areas exclusively composed of amorphous silica. This can be best recognized in clinochlore inclusions embedded in areas of amorphous silica with only traces of chromite NPs (Fig. 2).

DISCUSSION

This study presents petrographic associations observed only at the nanoscale with mineral relationships that were not expected, and which dictate how these minerals geochemically behave in a weathering environment. This has important environmental consequences in the weathering of chromitite ore, even though the two samples we observed are from two distinct geologic environments (an ultramafic-mafic intrusive complex versus a metamorphosed ophiolite at a convergent boundary).

Specifically, we demonstrate the occurrence of chromite NPs in silicate minerals associated with chromite. Although the areas investigated in this study with FIB/microtome sectioning/TEM are physically limited, our observations provide an alternative model for the speciation of Cr in minerals of the serpentine and chlorite groups; i.e..the common assumption is that Cr replaces Al in octahedral coordination in silicates such as Cr-rich chlorites (Lapham, 1958) although the structural incorporation of Cr into the octahedral sites of boehmite, (orthorhombic g-AlOOH)has been recently questioned by Chatterjee, et al. (2016).

The ratio between chromite NPs and Cr structurally incorporated into the observed silicates is difficult to estimate as the NPs are finely distributed within their matrices. However, it can be noted that the number of chromite NPs observed qualitatively tracks with the total concentration of Cr in the silicates, with a higher number of NPs in the clinochlore (per area in the image) from the Black Thor deposit (Fig. 1b; average 3 wt% Cr) versus in the lizardite from the Mistake Mine (Fig. 1f, average 1 wt% Cr).

Agglomeration, release and crystal growth through particle attachment

The occurrence of larger chromite aggregates in the chromitite sample from California and the occurrence of chromite fragments of different orientations and sizes within these aggregates (Figures S8, S10) suggest agglomeration of chromite NPs and the growth of chromite through particle attachment (CPA, De Yorero et al. 2015). Agglomeration of NPs occurs when Brownian diffusion brings particle surfaces into contact with each other and attractive Van der Waals (vdW) forces are greater than repulsive electrostatic double layer (EDL) forces (theory of Derjaguin, Landau, Verwey, and Overbeek; or DLVO) (Hotze et al. 2010, De Yorero et al. 2015).

Dissolution of the chromitite ore under acidic conditions resulted in the formation of amorphous silica in areas formerly composed of clinochlorite. The formation of the silica has been identified on the surfaces of numerous silicate minerals after dissolution experiments under acidic conditions as well as in acidic mine tailings and soils (*e.g*. Teng *et al*., 2001; Hochella *et al*., 2005; Schindler *et al*., 2012; Schindler and Hochella 2015, 2016) and has been attributed to either a leaching-proton-exchange process (*e.g.* Schweda *et al.*, 1997) or an interfacial dissolution-reprecipitation (Hellmann *et al.,* 2012). Either way, the formation of amorphous silica during the non-stoichiometric dissolution of clinochlore under acidic conditions has resulted in the release of chromite NPs. The NPs are no longer visible (Fig. 2), and EDS shows that the Cr concentration in the silica is significantly lower than in the former silicate.

Mobility and retention of NPs are mainly controlled by interactions between other suspended particles, and between particles and larger mineral surfaces. Retention of NPs is for example favored when mineral surfaces and NPs have opposing charges (Hotze et al. 2010), which was not the case during the dissolution experiments under acidic conditions (pH = 2.5) where the surfaces of amorphous silica (point of zero charge, pH_{pzc} = 4.1, Kosmulski 2009) and chromite (pH_{pzc} = 6.5, Souza et al. 2012) had both strong positive charges. This is in accordance with the lower abundance of chromite NPs in the amorphous silica than in clinochlore (Fig. 2).

IMPLICATIONS

Chromium-bearing silicates such as minerals of the serpentine and chlorite group are more susceptible to weathering than chromite and as such the solubility and dissolution kinetics of these minerals control the amount of Cr released to the environment. Chromium can be structurally incorporated into these minerals, replacing Al^{3+} in octahedral and tetrahedral coordination. The results of this study show that Cr^{3+} can also occur as chromite NPs in silicates and that these NPs can be released or dissolved during the non-stoichiometric dissolution of the silicates. The release of chromite NPs rather than Cr^{3+} aqueous species during alteration of Cr-bearing silicates would have a large impact on the fate of Cr^{3+} in the environment as the behaviour of NPs is predominantly governed by the interaction between charged mineral surfaces. For example, common alteration products of Fe-rich minerals of the chlorite and serpentine groups under near neutral pH conditions are Fe-hydroxides (Murakami et al. 1996). These minerals would be able to retain chromite NPs due to their large surface area (Fandeur et al. 2009), especially in the pH range of 7 to 8, where the surfaces of chromite NPs and of some Fe-hydroxides can be negatively and positively charged, respectively (Cornell and Schwertmann 1996).

The release of chromite NPs during the weathering of silicate minerals associated with chromite would also result in (a) lower concentrations of dissolved Cr^{3+} aqueous species (than

206 expected from the total concentrations of Cr in the silicates) and thus in lower rates of Cr^{3+}-
207 hydroxide formation if conditions favoured that, and (b) lower oxidation rates of Cr^{3+} to Cr^{6+} as
208 this would require either the dissolution of the NPs or the oxidation of Cr^{3+} species on the
209 surfaces of the NPs, processes that would be most likely the rate-limiting steps for the oxidation
210 of Cr^{3+} to Cr^{6+} in aqueous solution. Future risk assessments of Cr-contaminated soils, tailings
211 and mine waste dumps must therefore include an estimate on the abundance of chromite NPs
212 in Cr-rich silicates.

213 **ACKNOWLEDGEMENTS**

214 This work was supported by a Best of Science Award from the Ministry of Environment and
215 Climate Change of Ontario to MS, as well as by the Virginia Tech National Center for Earth and
216 Environmental Nanotechnology Infrastructure (NanoEarth), a member of the National
217 Nanotechnology Coordinated Infrastructure (NNCI) funded by NSF (ECCS 1542100). We like to
218 thank Eugene Ilton, and an anonymous reviewer for their constructive comments and Associate
219 Editor David Singer for handling the paper. We also like to thank Christopher Winkler, James
220 Tuggle, and the Nanoscale Fabrication and Characterization Laboratory, a portion of the
221 Institute for Critical Technology and Applied Science at Virginia Tech.

222

223 **References**

224 Bartlett, R.J. and James, B.R. (1979) Behavior of chromium in soils: III. Oxidation. Journal of
225 Environmental Quality 8, 31–35.
226 Chatterjee,S., Conroy, M.A., Smith,F.N., Jung, H.J., Wang, Z., Peterson,R.A. Huq, A., Burtt,
227 D.G., Ilton, E.S.and Buck, E.S. (2016) Can Cr(III) substitute for Al(III) in the structure of
228 boehmite? RSC Advances, 6, 107628–107637
229 Coleman, R.G. (1996) New Idria Serpentinite: A land management dilemma. Environmental and
230 Engineering Geoscience, 2, 9-22.

231 Cornell, R.M. and Schwertmann, U. (1996) The iron oxides: structure, properties, reactions,
232 occurrences and uses. VCH Verlagsgesellschaft, New York, USA.
233 Derjaguin, B.V. and Landau. L. (1941) Theory of the stability of strongly charged lyophobic sols
234 and of the adhesion of strongly charged particles in solutions of electrolytes. Acta
235 Physico Chimica URSS, 14, 633–662.
236 De Yoreo, J.J., Gilbert, P.U.P.A., Sommerdijk, N. A. J. M., Penn, R.L., Whitelam, S., Joester, D.,
237 Zhang, H., Rimer, J.D., Navrotsky, A., Banfield, J.F., Wallace, A.F., Michel, F.M.,
238 Meldrum, F.C., Cölfen, H., and Dove, P.M. (2015) Crystallization by particle attachment
239 in synthetic, biogenic, and geologic environments. *Science*, 349, 498.
240 Eary, L.E. and Rai, D., (1987) Kinetics of chromium(III) oxidation to chromium(VI) by reaction
241 with manganese dioxide. Environmental Science and Technology 21, 1187–1193.
242 Fandeur, D., Juillot, F., Morin, G., Olivi, L., Cognigni, A., Ambrosi, J.P., Guyot, F. and Fritisch, E.
243 (2009) Synchrotron-based speciation of chromium in an Oxisol from New Caledonia:
244 importance of secondary Fe-oxyhydroxides. American Mineralogist 94, 710–719.
245 Fendorf, S.E. (1995) Surface reactions of chromium in soils and waters. Geoderma 67, 55–71.
246 Hellman R., Wirth, R., Daval, D., Barnes, J-P., Penisson, J-M., Tisserand, D., Epicier, T., Florin,
247 B. and Hervig, R.L. (2012) Unifying natural and laboratory chemical weathering with
248 interfacial dissolution–reprecipitation: A study based on the nanometer-scale chemistry
249 of fluid–silicate interfaces. Chemical Geology 280, 1-2.
250 Hochella M.F., Jr., Moore J.N., Putnis C., Putnis A., Kasama T., and Eberl D.D. (2005) Direct
251 observation of heavy metal-mineral association from the Clark Fork River Superfund
252 Complex: Implications for metal transport and bioavailability. Geochimica et
253 Cosmochimica Acta, 69, 1651-1663.
254 Hotze, E.M. Phenrat, T. and Lowry, G.V. (2010) Nanoparticle Aggregation: Challenges to
255 Understanding Transport and Reactivity in the Environment. Journal of Environmental
256 Quality 39, 1909–1924.

Hseu, Z.Y. and Iizuka, Y. (2013) Pedogeochemical characteristics of chromite in a paddy soils derived from serpentinites. Geoderma 202–203, 126–133.

Izbicki, J.A., Ball, J.W., Bullen, T.D. and Sutley, S. (2008) Chromium, chromium isotopes and selected traced elements, western Mojave Desert, USA. Applied Geochemistry 23, 1325–1352.

Laarman, J.E. (2013) Detailed metallogenic study of the McFaulds lake chromite deposits, Norther Ontario, Ph.D. thesis, The University of Western Ontario, pp. 494,

Murakami, T. Isobe, H., Sato, T. and Ohnuki T. (1996) Weathering of chlorite in a quartz-chlorite schist: I. Mineralogical and chemical changes. Clays and Clay Minerals 44, 244-256.

Oze, C., Bird, D.K. and Fendorf, S. (2007) Genesis of hexavalent chromium from natural sources in soil and groundwater. Proceeding of the National Academy of Science USA 104, 6544–6549.

Oze, C., Fendorf, S., Bird, D.K. and Coleman, R.G. (2004) Chromium geochemistry in serpentinized ultramafic rocks and serpentine soils from the Franciscan complex of California. American Journal of Sciences 304, 67–101.

Kamaludeen, S. P. B. Megharaj, M., Juhasz, A.L., Sethunathan, N. and Naidu, R. (2003) Chromium–Microorganism Interactions in Soils: Remediation Implications. Reviews of Environmental Contamination and Toxicology 178, 93–164.

Kosmulski, M. (2009) pH-dependent surface charging and points of sero charge. IV. Update and new approach. Journal of Colloid and Interface Science 337, 439-448.

Lapham, D. M. (1958) Structural and chemical variation in chromium chlorite: American Mineralogist 43, 921-956.

Morrison J.M., Goldhaber, M.B., Mills C.T., Breit G.N., Hooper, R.L., Holloway, J.M., Diehl, S.F. and Ranville, J.F. (2015) Weathering and transport of chromium and nickel from serpentinite in the Coast Range ophiolite to the Sacramento Valley, California, USA Applied Geochemistry 61, 72–86.

283 Plathe, K.L., von der Kammer, F., Hassellöv, M., Moore, J., Murayama, M., Hofmann, T., and
284 Hochella, Jr. M.F. (**2010)** Using FlFFF and a TEM to determine trace metal–nanoparticle
285 associations in riverbed sediment. *Environmental Chemistry 7*, 82.
286 Souza, R.F., Paulo R.G. Brandão, P.R.G. and Paulo, J.B.A. (2012) Effect of chemical
287 composition on the ζ-potential of chromite. Minerals Engineering 36–38, 65–74.
288 Schindler, M., Durocher, J., Abdu, Y., and Hawthorne, F.C. (2009) Hydrous Silica Coatings:
289 Occurrence, Speciation of Metals, and Environmental Significance. Environmental
290 Science and Technology 43, 8775–8780.
291 Schindler, M., and Hochella, M.F. (2015) Soil memory in mineral surface coatings:
292 environmental processes recorded at the nanoscale. Geology 43, 415–418.
293 Schindler, M.; Hochella, Jr. M.F. (2016) Nanomineralogy is a new dimension in understanding
294 illusive geochemical processes in soils: The case of low solubility index elements.
295 Geology 44, 515-519.
296 Schweda, P., Sjöberg L., and Södervall U. (1997) Near-surface composition of acid-leached
297 labradorite investigated by SIMS. Geochimica et Cosmochimica Acta 61, 1985–1994.
298 Teng, H.H., Fenter P., Cheng, L., and Sturchio, N.C. (2001): Resolving orthoclase dissolution
299 processes with atomic force microscopy and X-ray reflectivity. Geochimica et
300 Cosmochimica Acta 65**,** 3459–3474.
301 Verwey, E., Overbeek, J. and van Nes. K. (1948) The theory of the stability of liophobic colloids:
302 The interaction of sol particles having an electric double layer. Elsevier, Amsterdam.
303 Weaver R.M. and Hochella, M.F. Jr. (2003) The reactivity of seven Mn-oxides with Cr^{3+}aq: A
304 comparative analysis of a complex, environmentally important redox reaction. American
305 Mineralogist 88, 2016–2027.
306 Weston R. and Shinkle D.A. (2013) Geology and stratigraphy of the Black Thor and Black Label
307 chromite deposits, James Bay Lowlands, Ontario, Canada 12th SGA Biennial Meeting
308 Proceedings.

309 Wood, W.W., Clark, D., Imes, J.L. and Councell, T.B. (2010) Eolian transport of geogenic
310 hexavalent chromium to ground water. Ground Water 48, 19–29.
311 Yang, Y., Colman, B.P., Bernhardt, E.S., and Hochella Jr. M.F. (**2015)** Importance of a
312 nanoscience approach in the understanding of major aqueous contamination senarios:
313 case study from a recent coal ash spill. Environmental Science and Technology 49,
314 3375-3382.

315

316 **Figure Captions**

317 Figure 1 (a) Back-scattered electron image of the chromitite ore from the Black Thor deposit,
318 Northern Ontario Canada, indicating cumulus aggregates of chromite (chr) grains with interstitial
319 clinochlore (chl); (b) TEM image of chromite nanoparticle (black dots) in clinochlore matrix
320 (grey); (c) High-resolution TEM image of a chromite nanoparticle in the clinochlore matrix
321 displaying lattice fringes with d = 2.05 Å (highlighted with solid white lines); (d) SAED pattern of
322 the clinochlore matrix with diffraction spots and rings corresponding to a clinochlore single
323 crystals and chromite nanoparticles, respectively; (e) TEM image of the sample from the
324 Mistake Mine in California depicting typical morphological features of lizardite (liz); (f) TEM
325 image of chromite nanoparticles within the lizardite matrix; a fast fourier transform (FFT) image
326 of the lattice fringes in this image is shown in the lower right corner, with the spotted ring
327 corresponding to the (400) lattice spacing of chromite.

328

329 Figure 2 Images of a treated sample after the dissolution experiment with a sulfuric acid bearing
330 solution; (a) Image in STEM mode indicating the occurrence of clinochlore fragments within an
331 amorphous silica matrix (encircled); (b) TEM image indicating occurrence and absence of
332 chromite nanoparticles in the clinochlore fragment and silica matrix; (c) chemical distribution
333 maps for Si (red) and Cr (green) indicating the absence of Cr in the silica matrix, respectively;
334 (d)-(e) chemical distribution maps for (d) Si (red), Cr (green) and Mg (blue) and (e) Cr (green)

indicating a higher abundance of Cr (green) in clinochlore fragments (violet) than in the silica matrix (red).

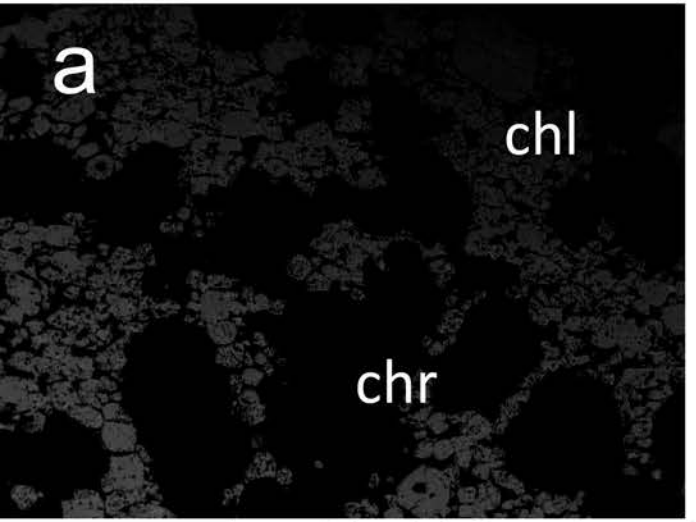

Black Thor deposit

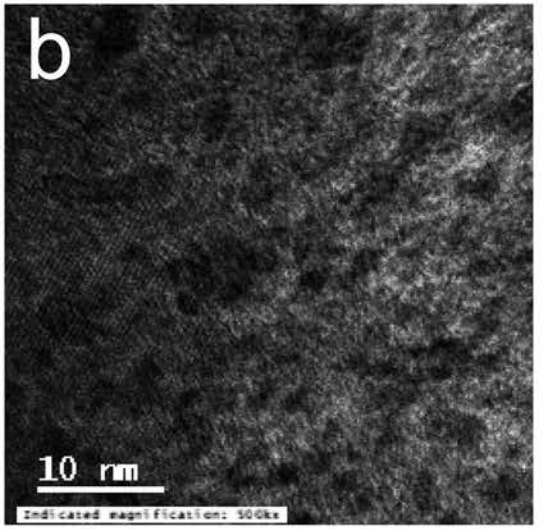

Black Thor deposit

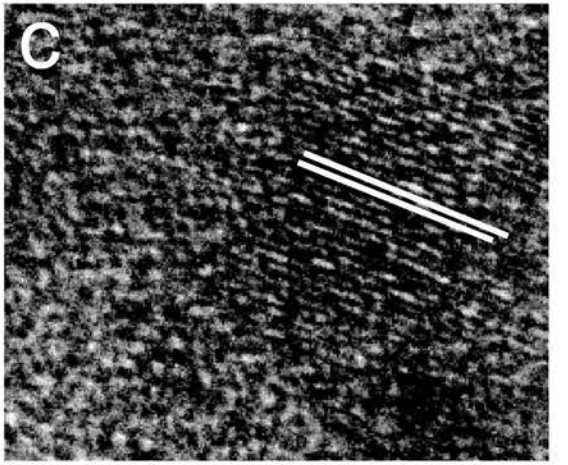

d = 2.05 Å (400) —— 1 nm

Black Thor deposit

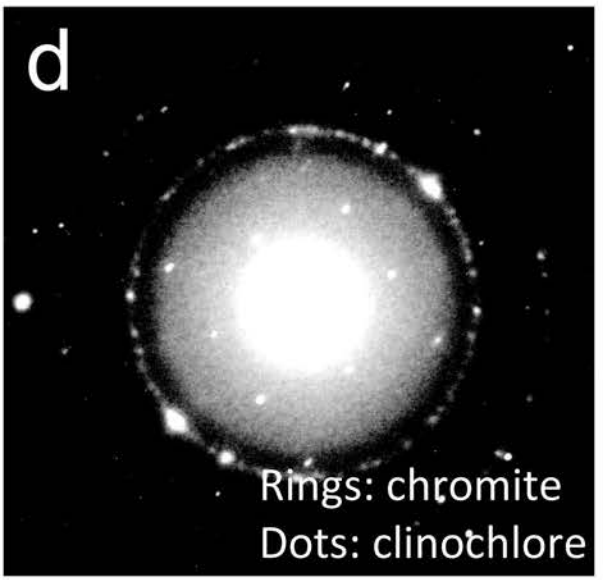

Black Thor deposit

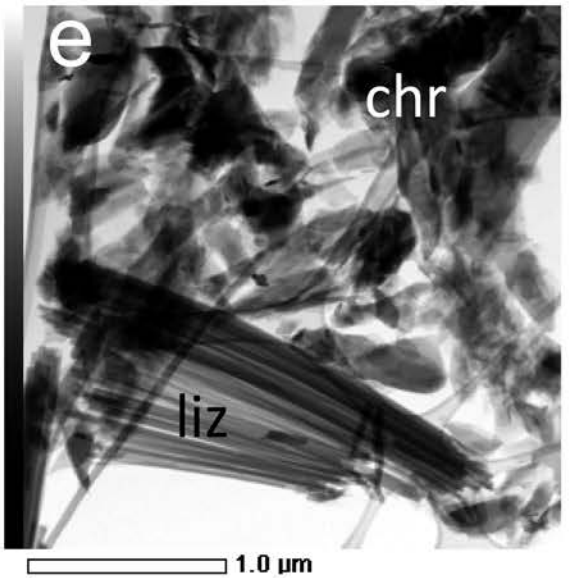

Mistake Mine

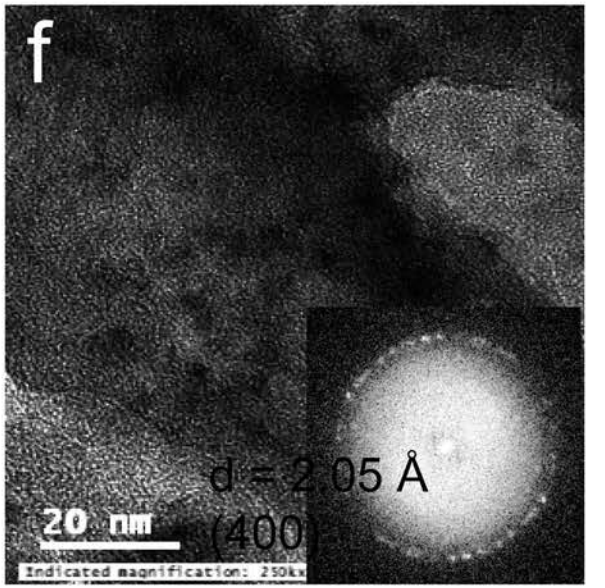

Mistake Mine

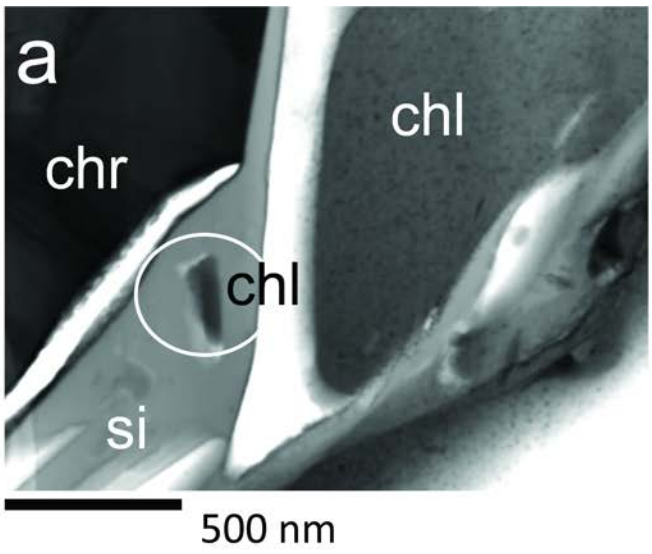
a
chr
chl
chl
si
500 nm

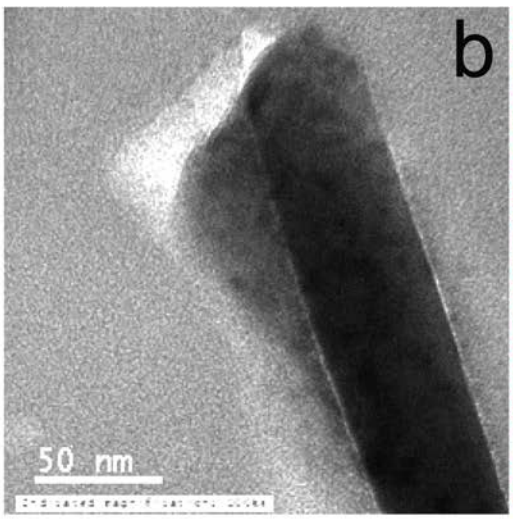
b
50 nm

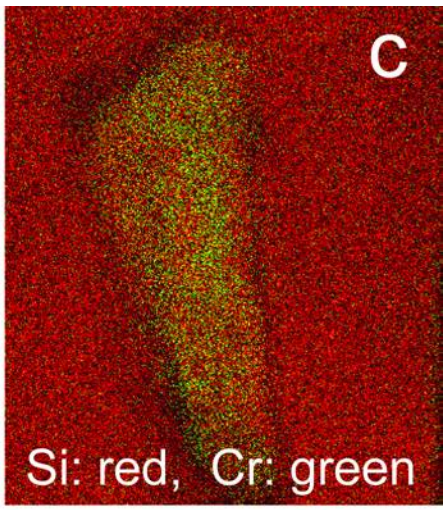
c
Si: red, Cr: green

50 nm

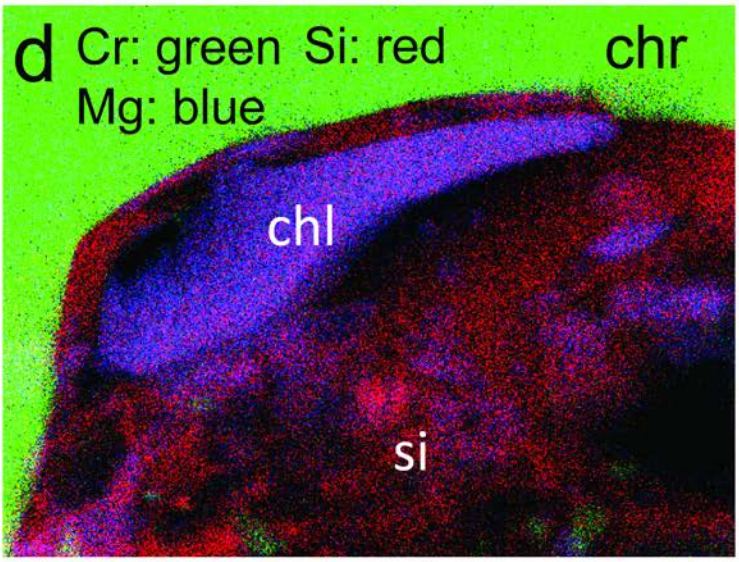
d
Cr: green Si: red
Mg: blue
chr
chl
si
0.5 µm

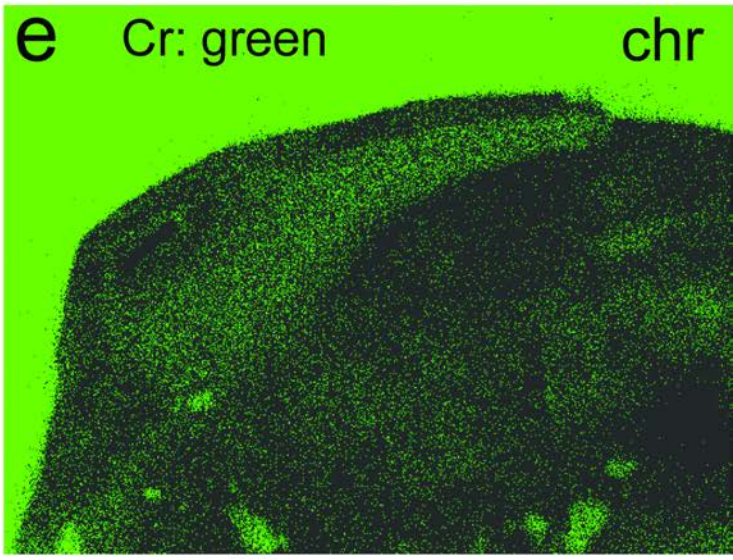
e
Cr: green
chr
0.5 µm